ARTICLES

Journal of Semiconductors
(2019) 40, 092002
doi: 10.1088/1674-4926/40/9/092002

A gate-free MoS_2 phototransistor assisted by ferroelectrics

Shuaiqin Wu[1, 2], Guangjian Wu[1], Xudong Wang[1], Yan Chen[1], Tie Lin[1, 2], Hong Shen[1, 2], Weida Hu[1, 2, †], Xiangjian Meng[1, 2], Jianlu Wang[1, 2, †], and Junhao Chu[1, 2]

[1]State Key Laboratory of Infrared Physics, Shanghai Institute of Technical Physics, Chinese Academy of Sciences, Shanghai 200083, China
[2]University of Chinese Academy of Sciences, Beijing 100049, China

Abstract: During the past decades, transition metal dichalcogenides (TMDs) have received special focus for their unique properties in photoelectric detection. As one important member of TMDs, MoS_2 has been made into photodetector purely or combined with other materials, such as graphene, ionic liquid, and ferroelectric materials. Here, we report a gate-free MoS_2 phototransistor combined with organic ferroelectric material poly(vinylidene fluoride-trifluoroethylene) (P(VDF-TrFE)). In this device, the remnant polarization field in P(VDF-TrFE) is obtained from the piezoelectric force microscope (PFM) probe with a positive or negative bias, which can turn the dipoles from disorder to be the same direction. Then, the MoS_2 channel can be maintained at an accumulated state with downward polarization field modulation and a depleted state with upward polarization field modulation. Moreover, the P(VDF-TrFE) segregates MoS_2 from oxygen and water molecules around surroundings, which enables a cleaner surface state. As a photodetector, an ultra-low dark current of 10^{-11} A, on/off ration of more than 10^4 and a fast photoresponse time of 120 μs are achieved. This work provides a new method to make high-performance phototransistors assisted by the ferroelectric domain which can operate without a gate electrode and demonstrates great potential for ultra-low power consumption applications.

Key words: TMDs; MoS_2 phototransistor; P(VDF-TrFE); PFM; ultra-low power consumption

Citation: S Q Wu, G J Wu, X D Wang, Y Chen, T Lin, H Shen, W D Hu, X J Meng, J L Wang, and J H Chu, A gate-free MoS_2 phototransistor assisted by ferroelectrics[J]. *J. Semicond.*, 2019, 40(9), 092002. http://doi.org/10.1088/1674-4926/40/9/092002

1. Introduction

Two-dimensional (2D) materials have attracted extensive attention all over the world in past decades. More and more new 2D materials have been found and novel device structures emerge in endlessly[1–5]. Since atoms are arranged by ionic bonds or covalent bonds closely in one layer, it is a weak van der Waals force that combines the atomically thin layers in 2D materials. So far, 2D materials, especially transition metal dichalcogenides (TMDs), have been widely used in developments of photodetectors due to the diversity of bandgaps[6]. Graphene, as the first 2D material to be found, owns a special and unique conic band structure and can keep stable in an ambient environment, is supposed to be utilized in photodetectors[7, 8]. However, it is hard for graphene to defined on and off-state for its zero bandgap. Molybdenum disulfide (MoS_2), which possesses a various band gap (1.2–1.8 eV) with different layers, is regarded as an alternative material for graphene to avoid such a predicament[9]. There have been many photodetectors using MoS_2 as the channel material and gain a high responsibility of 5.75×10^3 A/W[10], a high detectivity of 10^3 J[11] and a broadband photodetection of 500–1100 nm[12]. The mechanical exfoliation method, which was invented by A. Geim and K. Novoselov[13], has become a traditional method to obtain atomic and few-layer-thick 2D materials. However, such a method will introduce a significant density of surface defects and affect the contacts, dielectrics and channel performance of exfoliated 2D materials[14]. Additionally, it has been reported that oxygen, water molecule, exfoliation residues and sulfur vacancies can facilitate charge trapping process and enhance the hysteresis in MoS_2-based field-effect transistor[15]. Therefore, the release and capture of photo-generated carriers may be affected and thus lead to a slow response speed in pure MoS_2 photodetector.

Furthermore, most of these phototransistors rely on a real metal gate to apply a gate voltage then to reduce the dark current, leading to leakage between source/drain and gate, but usually, it is difficult to reduce the dark current in a satisfying level[16, 17]. Apparently, a low dark current will contribute to obtain a high photocurrent on/off switching ratio in a photodetector. Utilizing the remnant polarization field of ferroelectric materials, such as $BiFeO_3$, $LiNbO_3$, and poly (vinylidene fluoride-trifluoroethylene) (P(VDF-TrFE)) to regulate the carrier concentration has been reported previously[18–20]. Among these ferroelectric materials, P(VDF-TrFE) remains stable even under atmosphere condition[21]. Moreover, P(VDF-TrFE) covering MoS_2 completely can help to passivate or encapsulate trap states on the surface by the fluorine atom or hydrogen atom[22].

Here, we report the fabrication and operation of a gate-free MoS_2 phototransistor utilizing the remnant polarization field of P(VDF-TrFE) to modulate the carrier concentration in MoS_2. Instead of a metal gate, piezoelectric force microscopy (PFM) is employed to polarize P(VDF-TrFE) under resonant mode in this work. The ferroelectric field has two polarized directions with a local electric field of 10^9 V/m which is large enough to tune MoS_2 to completely depleted and accumu-

Correspondence to: W D Hu, wdhu@mail.sitp.ac.cn; J L Wang, jlwang@mail.sitp.ac.cn
Received 20 JULY 2019; Revised 13 AUGUST 2019.

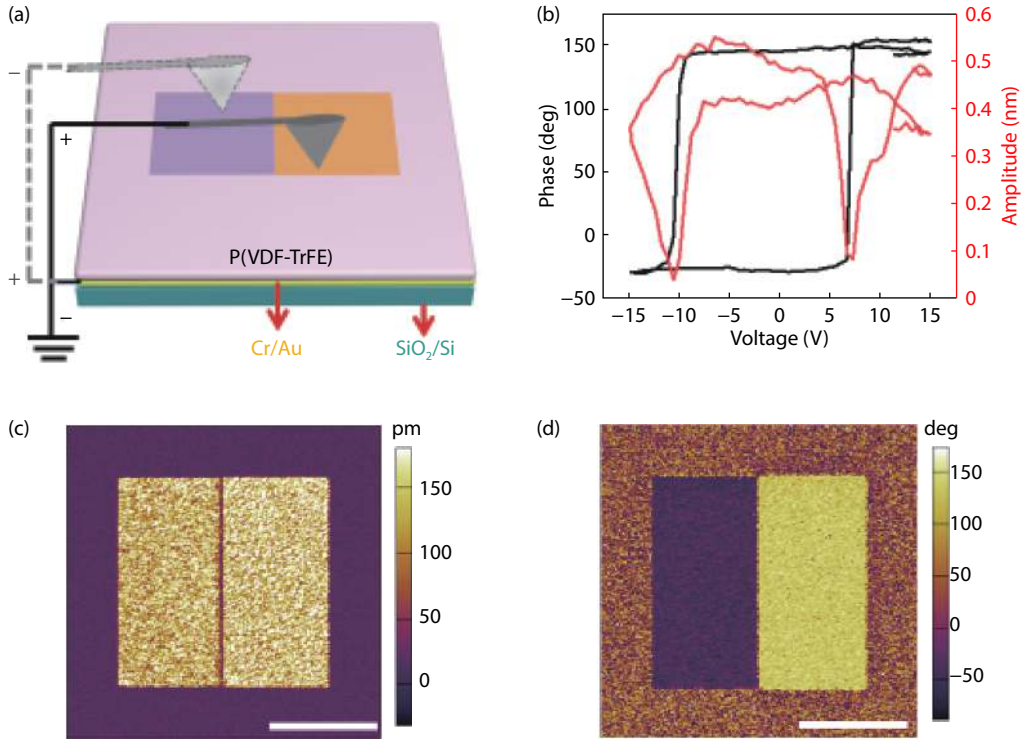

Fig. 1. (Color online) Ferroelectric polarization switching by PFM for 50 nm-thick P(VDF-TrFE) film. (a) Schematic of the operation for P(VDF-TrFE) polarization switching with PFM probe appling a positive or negative voltage. (b) The PFM amplitude (red) and phase (black) hysteresis loops during the switching process, scale bar is 10 μm. (c) Amplitude signal and (d) phase signal of the P(VDF-TrFE) film after writing half-to-half rectangle patterns with reversed DC bias, scale bar is 10 μm.

lated state[23, 24]. Therefore, the device structure is greatly simplified and the carrier concentration of MoS_2 is modulated without any external voltage, it means that a robust method to realize a phototransistor with ultra-low power consumption has raised in this work. Specifically, it is easy for us to select the direction based on the experience of previous reports[20, 22, 25, 26]. In this work, we applied a negative voltage to P(VDF-TrFE) through the tip of PFM to make the polarization direction of P(VDF-TrFE) upward, so that an extremely low dark current (approximately 10^{-12} A) can be achieved. Besides, since the MoS_2 is completely covered with ferroelectric material, where MoS_2 is isolated from atmospheric environment. Thus, the response time is dramatically improved (t_{rise} = 200 μs and t_{fall} = 120 μs), which is much faster than those exposed MoS_2 photodetectors reported previously[17, 27–29].

2. Experimental methods

PFM measurements were carried out at room temperature on a commercial atomic force microscope (Bruker Multimode 8, Camarillo, CA, USA). Positive and negative DC voltage were applied on P(VDF-TrFE) by a commercial silicon tip (Budget Sensors) covered with chromium/platinum under a contact resonance frequency of 0.7 MHz typically. When applied voltage by PFM probe, the sample will deform and cause the deflection of cantilever. Such a change can be measured to reflect the piezoelectric properties of the sample. For poly(vinylidene fluoride-trifluoroethylene) (P(VDF-TrFE)) copolymers used in this work, when a positive voltage applied on it, the domains will point down vertically while for negative voltage, the domains will point up vertically.

3. Results and discussion

3.1. Ferroelectric switching

Fig. 1(a) shows the schematic diagram of the operation for P(VDF-TrFE) polarization switching with PFM. The P(VDF-TrFE) film (50 nm) was spin-coated on the top of chromium/gold (Cr/Au) bottom electrode. The thickness of Cr and Au is 3 and 7 nm, respectively, which is prepared on a 285-nm-thick SiO_2 substrate by thermal evaporation. A DC bias is applied to the P(VDF-TrFE) through the PFM tip, and the bottom electrode is grounded. Fig. 1(b) shows the out-of-plane PFM signals of this P(VDF-TrFE) film. The amplitude signal represents the absolute magnitude of the local piezoelectric response, while the phase signal reveals the polarization direction in every individual domain[30]. A wonderful butterfly loop of the PFM amplitude signal and an apparent 180° transform of the phase signal were found. Figs. 1(c) and 1(d) display the amplitude signal and phase signal of this P(VDF-TrFE) film after writing half-to-half rectangle patterns with reversed DC bias (the amplitude of the DC bias is 15 V, and more details are illustrated in supplementary Fig. S1). As shown in Fig. 1(c), an obvious ferroelectric domain wall can be found in the middle of the two rectangular regions with opposite polarization directions. Besides, a clear 180° phase reversal also can be found between these two rectangular regions in Fig. 1(d), it can fully reveal the polarization switching characteristic of P(VDF-TrFE). To explore the magnitude of the ferroelectric field, we prepared the P(VDF-TrFE) capacitor with the same thickness. Its hysteresis loop indicates that the remnant polarization of P(VDF-TrFE) is approximately 10 μC/cm^2 (Supplementary Fig. S2). The ferroelectric field intensity can be calculated from $\sigma = \varepsilon\varepsilon_0 E$, where σ rep-

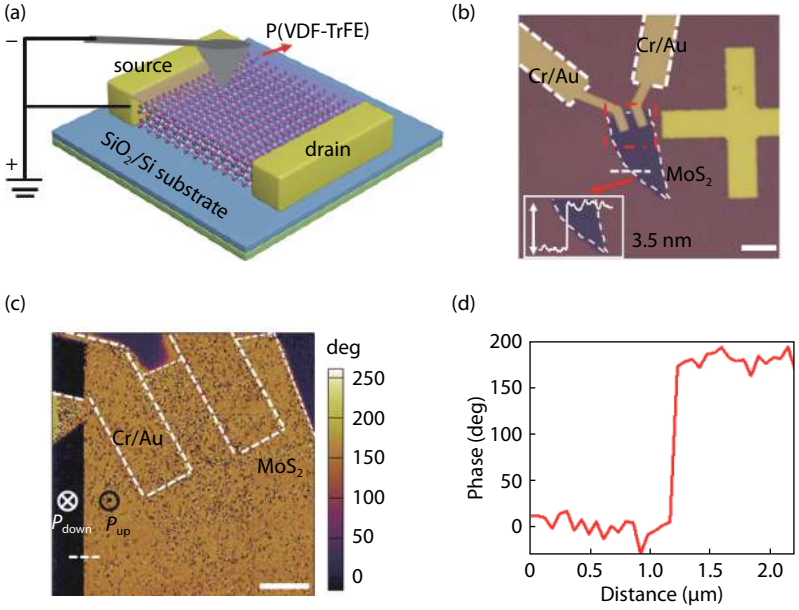

Fig. 2. (Color online) Structure illustration of the gate-free MoS_2 photodetector. (a) A 3D schematic of the device structure. (b) The optical image of the device, which includes a 3.5 nm MoS_2 and Cr/Au source and drain electrodes covered by 50 nm-thick P(VDF-TrFE) film, scale bar is 10 μm. (c) The PFM phase image of the device (red square part in (b)), two polarization states of P_{down} and P_{up} represent the opposite direction of the electric dipole moment in different parts (orange and black), scale bar is 3 μm. (d) Phase profile extracted along the white dashed line in (c), which demonstrated that the MoS_2 in the channel has a 180° phase difference with the other part.

resents the electric density at the surface of the ferroelectric film, ε is the dielectric constant of contact material, ε_0 is the permittivity of vacuum, and E is the electric field. In this work, the contact material is MoS_2 and its dielectric constant is approximately 4–6[31, 32]. Therefore, the local electric field applied to the MoS_2 is approximately 2.26×10^9 V/m which is strong enough to modulate the carrier concentration of MoS_2 and stay it in a totally depleted state.

Fig. 2(a) illustrates the configuration of the gate-free MoS_2 phototransistor. The MoS_2 was obtained by the Scotch tape-based mechanical exfoliation method, then transferred on the highly doped silicon substrate covered with a 285-nm-thick SiO_2. The source/drain electrode is Cr/Au which was prepared by electron beam lithography, thermal evaporation, and lift-off steps. The thickness of Cr and Au is 10 and 20 nm, respectively. Subsequently, the device was annealed at 200 °C for 2 h in an argon atmosphere. At last, 50 nm P(VDF-TrFE) film was spin-coated on the device and annealed at 135 °C for 2 h in an oven to enhance its crystallinity. The optical image of the device can be seen in Fig. 2(b) and the thickness of MoS_2 in this work is 3.5 nm measured by AFM (See the insert in Fig. 2(b)). The MoS_2 channel length is set to 5 μm. PFM was used to polarize P(VDF-TrFE) in different directions. As shown in Fig. 2(c), different regions of P(VDF-TrFE) on MoS_2 were polarized upward or downward. Fig. 2(d) shows the polarization phase signal extracted near the domain wall (Fig. 2(c)), a clear reversal of 180° can be found which reveals the MoS_2 is modulated by a downward polarization field.

3.2. Electrical properties and photoresponse properties

The electrical properties of the device were firstly studied. Fig. 3(a) shows the I_{sd}–V_{sd} characteristics under three different polarization states of P(VDF-TrFE). When a DC positive voltage is applied to the P(VDF-TrFE), the polarization direction is downward and the MoS_2 channel is in a carrier accumulation state (P_{down} state). Conversely, the polarization direction is upward and the MoS_2 channel is in a carrier depletion state (P_{up} state) when a DC negative voltage is applied. It can be obviously found that the channel current of the device in P_{down} state is larger than that in the fresh state by an order of magnitude, while the current in P_{up} state decreased into below 10^{-11} A, smaller than that in fresh state by more than 4 orders of magnitude. As a result, such an ultra-low dark current of the device in P_{up} state is very beneficial for photodetector operation. The sectional view of the device and the transport of carriers under two different polarization states (the P_{up} state and P_{down} state) are shown in Figs. 3(b) and 3(c). Fig. S3 presents the transfer characteristics of the device, it can reveal that MoS_2 used in this work is an intrinsic n-type semiconductor. As a result of electrostatic induction, when P(VDF-TrFE) is in P_{down} state, the electrostatic field from the remnant polarization makes the n-type MoS_2 channel in an accumulated state (Fig. 3(b)); when P(VDF-TrFE) is in P_{up} state, the electrostatic field changes into the opposite direction and the channel is in a depleted state (Fig. 3(c)). Fig. 3(d)–3(f) reveals the equilibrium band structure of MoS_2 when P(VDF-TrFE) is in three different polarization states. Fermi level (E_F) is defined as an energy level that the probability for an electron to take up is equal to 1/2. The Fermi level is close to conduction band for n-type semiconductors but close to valence band for p-type semiconductors. As shown in Fig. 3(d), the Fermi level of MoS_2 is close to the conduction band when P(VDF-TrFE) is in the fresh state. After applying a positive voltage to P(VDF-TrFE) by the PFM, a downward polarization field will be applied to the MoS_2. Then, the position of Femi level moves up and more electrons can take part in conduction, as shown in Fig. 3(e). In this case, if put the device under illumination and apply a drain bias to read the channel current, the photon-generated current will be covered up by the thermionic or tunneling current[33–35]. Conversely, once the

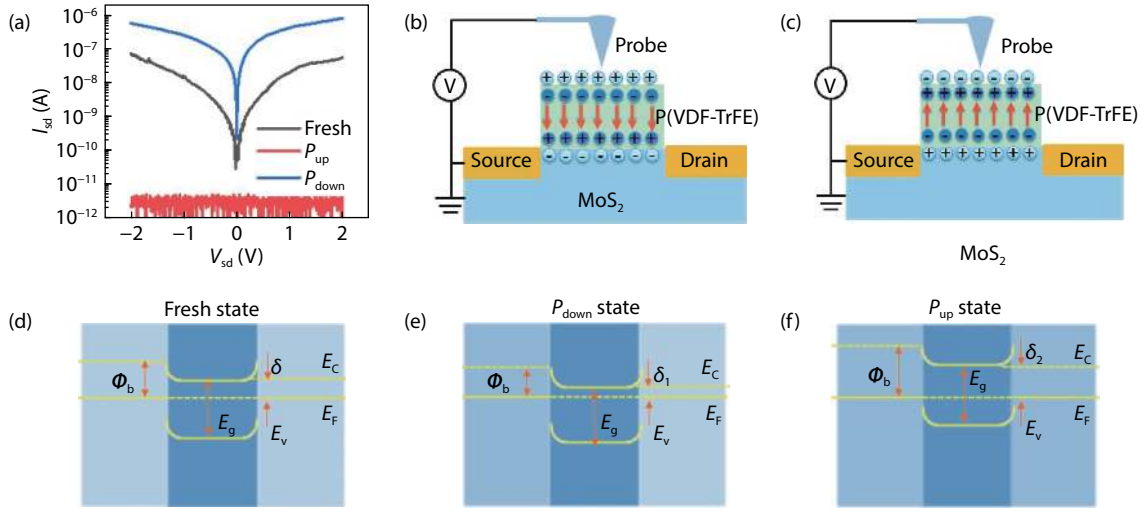

Fig. 3. (Color online) Electrical characteristics of the device with three different polarization states of P(VDF-TrFE). (a) The I_{sd}–V_{sd} characteristics of the device with three different polarization states of P(VDF-TrFE). These three polarization states are fresh (without polarization), P_{up} (upward polarization) and P_{down} state (downward polarization). (b) Sectional view of the device for illustrating the distribution of electron and hole under downward and (c) upward polarization state. (d–f) The energy band diagrams of the device with three polarization states at V_{sd} = 0 V. Φ_b is the Schottky barrier height, E_g is the energy gap of MoS_2, δ is the barrier height from conduction band to Fermi level.

MoS_2 is modulated by the upward polarization field, the position of Fermi level moves down and less electron can take part in conduction (Fig. 3(f)), and the photon-generated current will correspondingly hold dominate position.

Next, the optoelectronic performance of the device is comprehensively studied. A 520 nm laser is employed as the light source in these measurements. It is widely known that the photocurrent generation mechanism for MoS_2 photodetector is a photoconductive effect[27]. Specifically, under illumination conditions, the photo-generated electron-hole pairs give rise to the increase of free carrier concentration and cause an increase conductance of MoS_2[36]. Since the P(VDF-TrFE) can offer an ultra-high and stable polarization-induced electric field (approximate 10^9 V/m), the carrier concentration of MoS_2 can be modulated by changing the direction of polarization electric field. For a photodetector, we scanned P(VDF-TrFE) using PFM tip with a negative voltage (–15 V) to make the remnant polarization field upward, thus, the MoS_2 channel can maintain a totally depleted state and an ultra-low dark current can be achieved. As shown in Fig. 4(a), under the modulation of upward polarization field, the dark current is just on the order of several picoamperes, which is almost equivalent to the noise current caused by the external environment. When in illumination state, the current increases dramatically to several nanoamperes and becomes larger and larger as the laser power increases constantly. As shown in Fig. 4(b), under a 520 nm laser (P = 6.56 μW) incident, the device displays an extraordinarily stable and repeatable photocurrent on/off switching ratio of 10^4. A photocurrent map was obtained by scanning the incident light on the device and extracting the corresponding current. Fig. 4(c) demonstrates the photocurrent map of the device at V_{sd} = 1 V drain bias, the incident light wavelength is 520 nm and the light power is 0.28 μW. It can be clearly seen that the photocurrent occurs in the middle of the MoS_2 channel, and there is no photocurrent occurs between the MoS_2 and the source/drain electrode. It is shown that good ohmic contact has formed in the device instead of a Schottky contact.

The photoresponse time is another important parameter to evaluate the ability of photodetectors, which is defined as the time for the photocurrent switching from 10% to 90%. For our device, the photocurrent turns from off to on state is as fast as 200 μs (Fig. 4(d)), indicating a fleet generation of photo-generated electron–hole pairs in MoS_2. It takes 120 μs for the device to turns from on to off state (Fig. 4(e)), indicating a fast process of carrier recombination. The photoresponse speed of our device is faster than those intrinsic MoS_2 photodetectors (see Table 1)[17, 27–29]. Such a fast photoresponse speed is mainly contributed to the fact that P(VDF-TrFE) can inhibit those trap states on the surface of MoS_2 and enable photo-generated carriers to take full part in the conduction process[22, 37]. Organic polymer ferroelectric material P(VDF-TrFE) is proved to have a p-doped effect on 2D materials due to the C–F and C–Cl bonds[20]. Such a p-doped effect can help enhance the photoresponse properties of MoS_2 photodetector[17]. In detail, the p-doped effect induced by P(VDF-TrFE) decreases the surface defects of MoS_2. Thus, the carrier scattering is suppressed and the generation and transmission process of photo-generated carriers are faster than that exposed in the ambient air. Furthermore, the responsivity of the device to incident light at different wavelengths was evaluated. As shown in Fig. 4(f), the device has the highest responsivity under incident light of 600 nm, and has no photoresponse to incident light with a wavelength longer than 700 nm. Such a result is attributed to the absorption spectrum of MoS_2 and similar result has been reported in previous work[38].

4. Summary

In summary, we have fabricated a gate-free MoS_2 phototransistor assisted by ferroelectric domain. Under the modulation of remnant polarization field, the carrier concentration of the MoS_2 channel is completely depleted and the optoelectronic performance of the device is greatly enhanced. The dark current of the MoS_2 photodetector is reduced to the order of several picoamperes. The photoresponse time is also improved to 200 and 120 μs, which is much faster than those intrinsic MoS_2

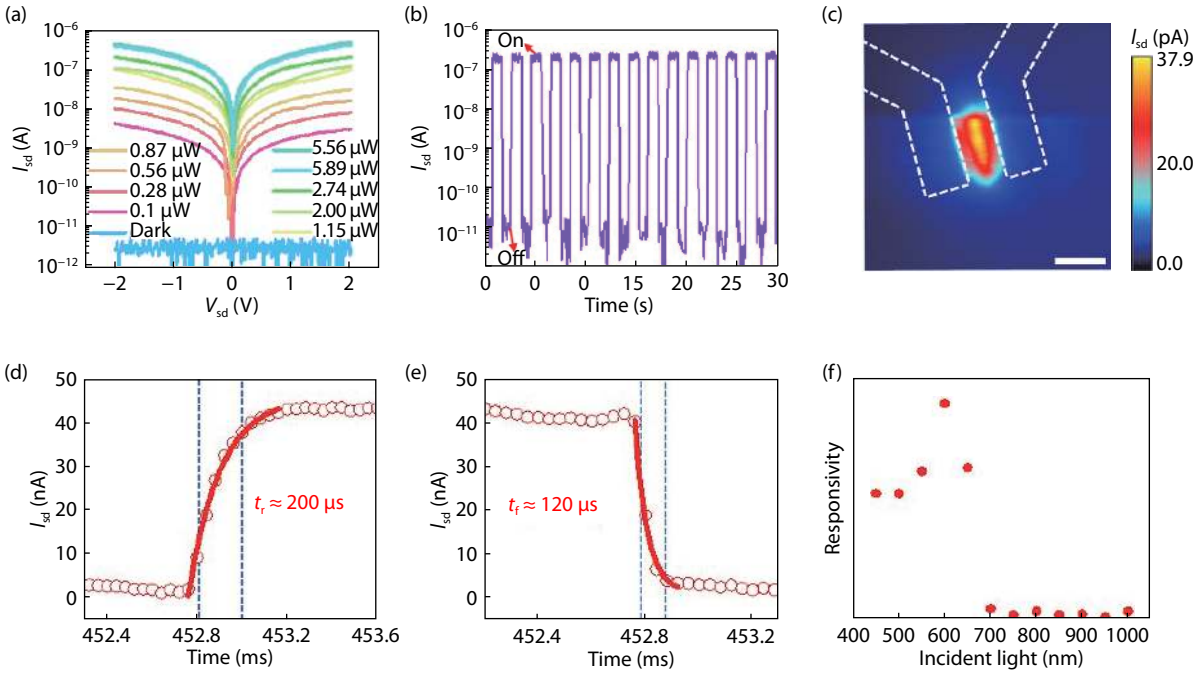

Fig. 4. (Color online) Optoelectronic properties of the device. (a) I_{sd}–V_{sd} curves of the device under dark and different power of incident light (520 nm). (b) photocurrent switching characteristic of the device with 520 nm laser illumination. The light power is 6.56 μW and V_{sd} = 1 V. (c) The photocurrent map of the device recorded at P_{up} state and V_{sd} = 1 V, the incident light power is 0.28 μW, scale bar = 3 μm. (d, e) The photocurrent rise and fall time extracted from a photocurrent switching cycle. (f) The photoresponse characteristic of the device under incident light with the different wavelengths but the same power.

Table 1. Photoresponse speed comparation between our device and other MoS_2-based photodetectors.

Description	Response time (s)	Wavelength (nm)	Gate voltage /Bias	Ref.
MoS_2–SiO_2–Si back gate	2	532	V_g = 100 V, V_{sd} = 5 V	[27]
MoS_2–SiO_2–Si back gate (CVD)	3	532	V_g = 40 V, V_{sd} = 1 V	[17]
MoS_2–Al_2O_3–ITO top gate	0.3	580	V_g = –9 V, V_{sd} = 1 V	[28]
MoS_2–SiO_2–Si back gate	0.05	488	V_g = 50 V, V_{sd} = 1 V	[29]
MoS_2–P(VDF-TrFE)	1.2×10^{-4}	520	V_g = 0 V, V_{sd} = 1 V	This work

photodetectors without P(VDF-TrFE). More importantly, such a gate-free MoS_2 phototransistor assisted by the ferroelectric domain embraces the ultra-low power consumption. Therefore, it provides a reliable way to develop 2D materials-based photodetectors with high-performance and ultra-low power consumption.

Acknowledgments

This work was partially supported by the Major State Basic Research Development Program (Grant Nos. 2016YFA0203900, 2016YFB0400801 and 2015CB921600), and Key Research Project of Frontier Sciences of Chinese Academy of Sciences (Nos. QYZDB-SSW-JSC016, QYZDY-SSW-JSC042). Strategic Priority Research Program of Chinese Academy of Sciences (XDPB12, XDB 3000000). Natural Science Foundation of China (Grant Nos. 61521001, 61574151, 61574152, 61674158, 61722408, 61734003 and 61835012), and Natural Science Foundation of Shanghai (Grant No. 16ZR1447600, 17JC1400302).

References

[1] Wang J. A novel spin-FET based on 2D antiferromagnet. J Semicond, 2019, 40(2), 020401

[2] Jiang W, Wang X, Chen Y, et al. Large-area high quality $PtSe_2$ thin film with versatile polarity. InfoMat, 2019, 1, 260

[3] Wu G, Wang X, Chen Y, et al. Ultrahigh photoresponsivity MoS_2 photodetector with tunable photocurrent generation mechanism. Nanotechnology, 2018, 29(48), 485204

[4] Liu L, Wang X, Han L, et al. Electrical characterization of MoS_2 field-effect transistors with different dielectric polymer gate. AIP Adv, 2017, 7(6), 065121

[5] Xue S, Zhao X L, Wang J L, et al. Preparation of $La_{0.67}Ca_{0.23}Sr_{0.1}MnO_3$ thin films with interesting electrical and magnetic properties via pulsed-laser deposition. Sci Chin Phys, Mechan, Astron, 2017, 60(2), 027521

[6] Wang J, Fang H, Wang X, et al. Recent progress on localized field enhanced two-dimensional material photodetectors from ultraviolet-visible to infrared. Small, 2017, 13(35), 1700894

[7] Son Y W, Cohen M L, Louie S G. Energy gaps in graphene nanoribbons. Phys Rev Lett, 2006, 97(21), 216803

[8] Meyer J C, Geim A K, Katsnelson M I, et al. The structure of suspended graphene sheets. Nature, 2007, 446(7131), 60

[9] Peelaers H, Van de Walle C G. Effects of strain on band structure and effective masses in MoS_2. Phys Rev B, 2012, 86(24), 241401

[10] Kang D H, Kim M S, Shim J, et al. High-performance transition metal dichalcogenide photodetectors enhanced by self-assembled monolayer doping. Adv Funct Mater, 2015, 25(27), 4219

[11] Wang L, Jie J, Shao Z, et al. MoS_2/Si heterojunction with vertically standing layered structure for ultrafast, high-detectivity, self-driven visible-near infrared photodetectors. Adv Funct Maters, 2015,

25(19), 2910
[12] Jariwala D, Sangwan V K, Wu C C, et al. Gate-tunable carbon nanotube-MoS_2 heterojunction pn diode. Proc Nat Acad Sci, 2013, 110(45), 18076
[13] Novoselov K S, Geim A K, Morozov S V, et al. Electric field effect in atomically thin carbon films. Science, 2004, 306(5696), 666
[14] Addou R, Colombo L, Wallace R M. Surface defects on natural MoS_2. ACS Appl Mater Interfaces, 2015, 7(22), 11921
[15] Di Bartolomeo A, Genovese L, Giubileo F, et al. Hysteresis in the transfer characteristics of MoS_2 transistors. 2D Mater, 2017, 5(1), 015014
[16] Kwon J, Hong Y K, Han G, et al. Giant photoamplification in indirect-bandgap multilayer MoS_2 phototransistors with local bottom-gate structures. Adv Mater, 2015, 27(13), 2224
[17] Zhang W, Huang J K, Chen C H, et al. High-gain phototransistors based on a CVD MoS_2 monolayer. Adv Mater, 2013, 25(25), 3456
[18] Wu C L, Chen J W. Chen C H, et al. A gate-free monolayer WSe_2 pn diode. APS Meeting Abstracts, 2018
[19] Baeumer C, Saldana-Greco D, Martirez J M P, et al. Ferroelectrically driven spatial carrier density modulation in graphene. Nat Commun, 2015, 6, 6136
[20] Yin C, Wang X, Chen Y, et al. A ferroelectric relaxor polymer-enhanced p-type WSe_2 transistor. Nanoscale, 2018, 10(4), 1727
[21] Tian B B, Wang J L, Fusil S, et al. Tunnel electroresistance through organic ferroelectrics. Nat Commun, 2016, 7, 11502
[22] Wang X, Wang P, Wang J, et al. Ultrasensitive and broadband MoS_2 photodetector driven by ferroelectrics. Adv Mater, 2015, 27(42), 6575
[23] Kufer D, Konstantatos G. Highly sensitive, encapsulated MoS_2 photodetector with gate controllable gain and speed. Nano Lett, 2015, 15(11), 7307
[24] Lee H S, Min S W, Park M K, et al. MoS_2 nanosheets for top-gate nonvolatile memory transistor channel. Small, 2012, 8(20), 3111
[25] Zhang E, Wang W, Zhang C, et al. Tunable charge-trap memory based on few-layer MoS_2. ACS Nano, 2014, 9(1), 612
[26] Zhao D, Katsouras I, Asadi K, et al. Switching dynamics in ferroelectric P (VDF-TrFE) thin films. Phys Rev B, 2015, 92(21), 214115
[27] Furchi M M, Polyushkin D K, Pospischil A, et al. Mechanisms of photoconductivity in atomically thin MoS_2. Nano Lett, 2014, 14(11), 6165
[28] Lee H S, Min S W, Chang Y G, et al. MoS_2 nanosheet phototransistors with thickness-modulated optical energy gap. Nano Lett, 2012, 12(7), 3695
[29] Li H, Wu J, Yin Z, et al. Preparation and applications of mechanically exfoliated single-layer and multilayer MoS_2 and WSe_2 nanosheets. Acc Chem Res, 2014, 47(4), 1067
[30] Gruverman A, Kalinin S V. Piezoresponse force microscopy and recent advances in nanoscale studies of ferroelectrics. J Mater Sci, 2006, 41(1), 107
[31] Chen X, Wu Z, Xu S, et al. Probing the electron states and metal-insulator transition mechanisms in molybdenum disulphide vertical heterostructures. Nat Commun, 2015, 6, 6088
[32] Santos E J G, Kaxiras E. Electrically driven tuning of the dielectric constant in MoS_2 layers. ACS Nano, 2013, 7(12), 10741
[33] Xie Y, Zhang B, Wang S, et al. Ultrabroadband MoS_2 photodetector with spectral response from 445 to 2717 nm. Adv Mater, 2017, 29(17), 1605972
[34] Lopez-Sanchez O, Lembke D, Kayci M, et al. Ultrasensitive photodetectors based on monolayer MoS_2. Nat Nanotechnol, 2013, 8(7), 497
[35] McCreary K M, Hanbicki A T, Robinson J T, et al. Large-area synthesis of continuous and uniform MoS_2 monolayer films on graphene. Adv Funct Mater, 2014, 24(41), 6449
[36] Long M, Wang P, Fang H, et al. Progress, challenges, and opportunities for 2D material based photodetectors. Adv Funct Mater, 2019, 29(19), 1803807
[37] Yin L, Wang Z, Wang F, et al. Ferroelectric-induced carrier modulation for ambipolar transition metal dichalcogenide transistors. Appl Phys Lett, 2017, 110(12)
[38] Choi W, Cho M Y, Konar A, et al. High-detectivity multilayer MoS_2 phototransistors with spectral response from ultraviolet to infrared. Adv Mater, 2012, 24(43), 5832